International Symposium
On Turbulence and Shear Flow
Phenomena (TSFP-9)
June 30 - July 3, 2015 *Melbourne, Australia*

EXPLORING THE INTERACTION OF RED BLOOD CELL ANALOGS WITH TURBULENCE USING PARTICLE TRACKING VELOCIMETRY

Saeed Rahgozar[1], **Giuseppe A. Rosi**[1], **Lucie Kaucky**[2], **Andrew Walker**[3], **David E. Rival**[1,2*]
1: Department of Mechanical and Materials Engineering, Queen's University, Kingston, ON, Canada.
2: Department of Mechanical Engineering, University of Calgary, Calgary, AB, Canada.
3: Department of Anesthesia, University of Calgary, Calgary, AB, Canada.
*Corresponding author: d.e.rival@queensu.ca

ABSTRACT

Particle Tracking Velocimetry (PTV) is performed in order to study the interaction of red blood cell analogs with turbulence. Super water absorbent deformable hydrogel beads are used to represent red blood cells (RBC) in different suspending fluids. Excellent optical matching is observed between the hydrogel beads and the suspending fluids. The results of PTV measurements show significant differences between the velocity patterns in the presence and absence of the hydrogel beads. However, the velocity patterns appear comparable between the different solutions. In order to analyze the detailed interaction of red blood cell analogs with turbulence, a new experiment has also been designed. An approximately homogeneous turbulent shear flow is generated in a large-scale tank by towing a shear generator consisting of a plane parallel-rod grid. In this large-scale experiment, large- and small-scale coherent structures will be investigated with and without RBC analogs in the absence of the complex wall effects.

INTRODUCTION

The study of blood flow dynamics is crucial to advancing biomedical devices and for understanding, diagnosing, preventing, and treating cardiovascular diseases (Ku, 1997). Moreover, modeling the transport of drugs through the cardiovascular system as well as planning cardiovascular surgery can be improved as our understanding of blood flow hemodynamics advances. Hemodynamics are well known to affect the development of atherosclerosis, a known mechanism in the development of heart disease that is a leading cause of death globally. In modeling the hemodynamics of large vessels where turbulence may occur, blood is most often assumed to behave as a homogenous, Newtonian fluid. However, blood presents as a viscoelastic suspension given the presence of red blood cells (RBC) that comprise approximately 50% of the total blood volume. Blood flow is a two-phase, pulsatile flow that may undergo transition from laminar to turbulent conditions in larger vessels such as the aorta or as it passes through artificial devices such as valves, and bypass tubing. The combination of turbulence and two-phase flow, which are two of the most challenging topics in fluid mechanics, leads to very complex interactions (Balachandar & Eaton, 2010).

Past work has demonstrated that particles in flow act to modify turbulence, either by augmentation or attenuation, depending on the individual and combined properties of the particles and fluid (Tanaka & Eaton, 2008; Balachandar & Eaton, 2010; Bellani *et al.*, 2012). In blood, it has been speculated that the prolonged laminar-like behaviour observed is due to RBC presence (Han *et al.*, 2001). Specifically, the packing and proximity of RBCs and their length scale relative to that of turbulent eddies is thought to affect the turbulent flow dynamics (Steinman, 2012). However, the mechanisms by which RBCs specifically modify turbulence in blood remain unclear. Furthermore, several researchers proposed that turbulent flow caused by medical cardiovascular devices may be responsible for RBC hemolysis (see for example Yen *et al.* (2014)) and platelet activation (Bluestein *et al.*, 1999).

Given this, the purpose of the present study is to analyze the interaction of RBCs with turbulent flow. Turbulent coherent structures, which are believed to be responsible for most of the momentum transfer are of particular interest. With exception of the visualization of Lagrangian coherent structures and a few studies on coherent vortices (Shadden & Taylor (2008); Vétel *et al.* (2009); Biasetti *et al.* (2011)), coherent structures have not been studied extensively in blood flow, partly because of the complexity of the flow and partly because the high-resolution measurement techniques like PIV (Particle Image Velocimetry) and PTV (Particle Tracking Velocimetry) are difficult to perform *in vivo*. The investigation of RBC behaviour in blood flow has primarily been limited to analytical and numerical models, however, the application of such models beyond the dynamics of a single-cell is challenging (Secomb *et al.*, 2007; Fedosov *et al.*, 2010; Mansour *et al.*, 2010). The numerical modelling of such a suspension, which consists of millions of colliding particles, specifically when applied to turbulent flow, becomes very computationally expensive (Cristini & Kassab, 2005). In the present study, Particle Tracking Velocimetry (PTV) is used to visualize the motion of tracer particles within an unsteady shear layer flow where deformable hydrogel beads, used to represent red blood cells, have been added to solutions of glycerine and water. The ultimate goal of the study is to analyze the interactions of RBC analogs with turbulent coherent structures. An example scenario of such interactions, inspired from the literature, is hypothesized in figure 1 (see for instance Adrian, 2007; Jiménez, 2013).

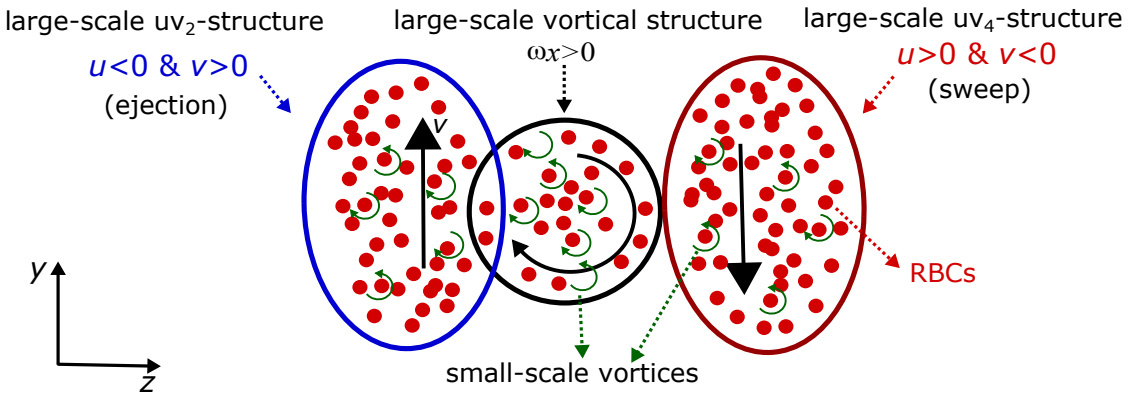

Figure 1. Schematic showing a possible scenario of red blood cell interacting with turbulent coherent structures in a cross-section of flow. It is hypothesized that kinematic and dynamic characteristics of small-scale vortices may be significantly altered in the presence of RBCs. RBCs might absorb turbulent kinetic energy of large-scale structures and dissipate it by elasticity and cell-cell interactions and/or transfer energy to small-scale structures. The large-scale uv-structures contribute most to the tangential Reynolds stress which is believed to be responsible for red blood cell hemolysis and platelet activation. Here, u, v are respectively the streamwise and wall-normal fluctuating components of velocity and ω_x is streamwise vorticity. uv_2 and uv_4 denote the second (ejection) and fourth (sweep) quadrant motions.

Figure 2. Super absorbent hydrogel beads upon complete saturation. Here an uncompressed bead relative to a compressed bead is shown, demonstrating the deformability of the hydrogel beads.

EXPERIMENTS

The experiments have been performed in two stages. Before conducting a large-scale experiment, a small-scale pilot study was carried out in a small water tank. In this first stage, the physical and optical adequacy of the hydrogel beads for PIV/PTV measurements in turbulent shear flow of different suspending fluids was assessed.

Preliminary Experiment

Super water absorbent hydrogel beads with a diameter of 1.0 cm (when fully saturated) are used to represent RBCs (see figure 2). The hydrogel beads are deformable with near-neutral buoyancy. The use of hydrogel particles in PIV measurements has been recently reported in the literature (e.g. Bellani *et al.*, 2012; Weitzman *et al.*, 2014). Initially, hydrogel beads at a concentration of approximately 50% by volume were added to a 110 Litre glass aquarium. A plate with a height (H) of 10 cm and a span of $3H$ was towed through quiescent fluid in the aquarium at a constant speed of 0.1 m/s (U_0) to generate a starting shear layer. The suspending fluids were tap water, and solutions of 30% (Glyc30) and 60% (Glyc60) by weight mixtures of aqueous glycerol equating to Reynolds numbers based on the plate height (H) of 10000, 5000 and 1000 respectively, that are commensurate with values of the cardiovascular system (see Stein & Sabbah, 1976). The density of the suspending fluids vary less than 15% while the viscosity of water and Glyc60 differs by more than an order of magnitude.

Images amenable to 2D-PTV analysis in both homogenous (without beads) and non-homogenous (with beads) shear flow were acquired using a Fastcam SA-4 camera (Photron, San Diego, CA, USA) at 125 Hz and a full resolution of 1024×1024 pixels. Neutrally buoyant 100 μm hollow glass spheres (Potters Industries, Carlstadt, NJ, USA) were added to the suspending fluids to serve as tracer particles. The addition of the hydrogel beads restricted the presence of tracer particles to the empty void between the beads. The tracer particles were illuminated using a solid-state, 532 nm continuous wave 1W laser (Dragon Lasers, Changchun, Jilin, China) with a sheet thickness of 1.5 mm at a distance of $0.75H$ along the span of the plate. Images of the illuminated tracer particles were acquired within a field of view (FOV) of approximately $1.2H \times 1.2H$ located a distance of $3H$ downstream from the near laser wall of the aquarium to mitigate potential wall effects on flow behaviour. Acquired images from 20 runs for the homogenous case and 100 runs for the non-homogenous case, to achieve an approximate equal number of tracked particles, were imported to DaVis 8.1.3 (LaVision GmbH, Goettingen, Germany) for PTV analysis. The raw images were brightened by a fixed factor and particles identified using a threshold limit to achieve a particle image density of approximately 0.005 particles per pixel (ppp) in the "non-bead" case (Cierpka *et al.*, 2013). Equivalent preprocessing of the images with beads generated an approximate particle density of 0.001 ppp. Lagrangian velocity data from the added tracer particles using a lower limit particle track length of two consecutive images were exported to MATLAB R2011a (Mathworks, Natick, MA, USA) for post-processing.

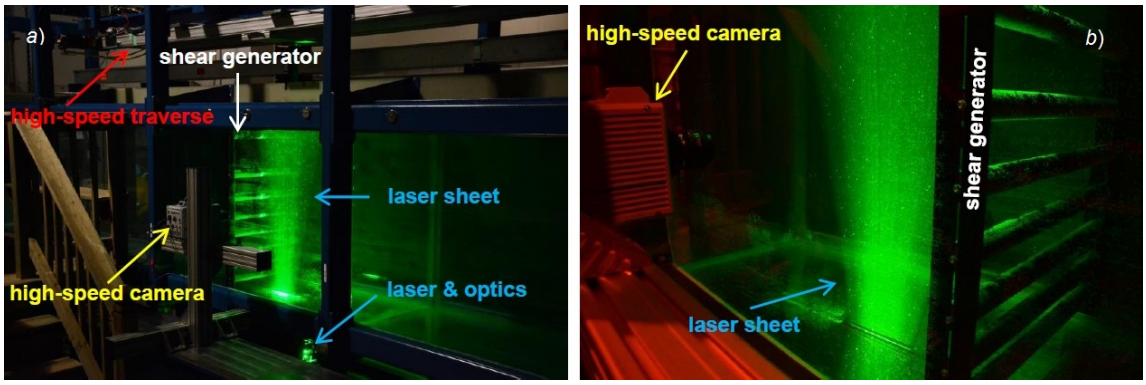

Figure 3. Experimental set-up in the large towing tank, (A) The shear generator and the high-speed traverse along with the PIV system, (B) A close-up of the shear generator.

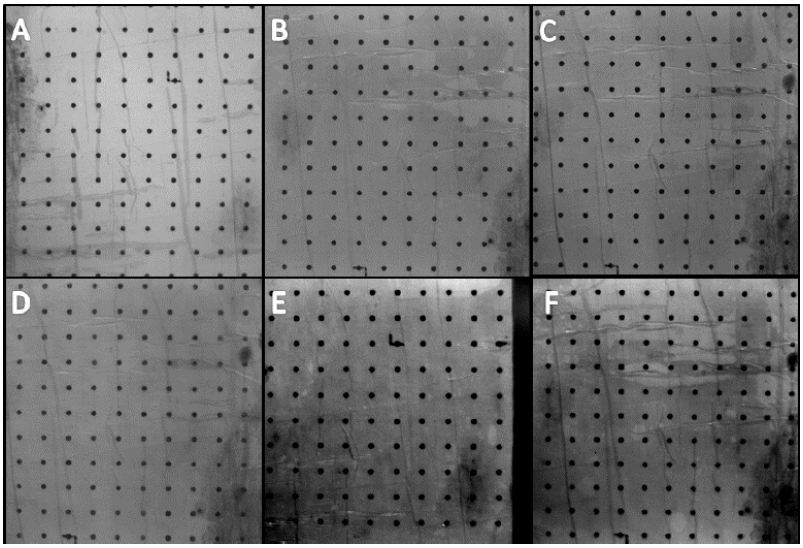

Figure 4. Images of the calibration target (with a 1×1 cm grid) placed at the laser sheet location. (A) water, (B) Glyc30, (C) Glyc60, (D) water with 50% beads, (E) Glyc30 with 50% beads and (F) Glyc60 with 50% beads. In homogenous and non-homogenous cases, thorough mixing of the solutions is confirmed by the absence of grid distortion.

New Experiment

The preliminary experiment serves to evaluate the adequacy of the hydrogel beads in terms of their optical matching to the suspending fluids for PIV/PTV measurements. Moreover, the experiment shows qualitatively that the presence of the hydrogel beads can significantly modify the structure of the flow. However, detailed analysis of turbulent flow in the presence of the RBC analogs demands to scale up the experiment in terms of the length-scale ratio between the RBC analogs and the shear flow in order to more accurately represent *in vivo* arterial blood flow. The large-scale turbulent shear flow allows for the characterization of turbulent statistics while permitting the analysis of the temporal and spatial characteristics of coherent structures using PIV/PTV techniques. On the other hand, the presence of the hydrogel beads limits the use of a water tunnel since the fluid mixture can not be circulated with pumps. A towing tank is thus a reasonable choice for the goal of the present study. The towing tank should be large enough with respect to the size of the test section to ensure negligible endwall effects. With these considerations in mind, a new set-up is designed in a large towing tank with dimensions $8 \times 1 \times 1$ m^3, as shown in figure 3. An approximately homogeneous turbulent shear flow is generated in the tank by towing a shear generator consisting of a plane parallel-rod grid of uniform rod diameter with non-uniform spacing (Owen & Zienkiewicz, 1957). A high-speed traverse system tows the shear generator in the center of the towing tank at speeds up to 1 m/s over a maximum distance of 4 m. By changing the arrangement of rods and the speed of the traverse, different shear rates can be generated. The glass windows allow for imaging with the aforementioned high-speed camera and laser (see figure 3). This large-scale experiment allows us to detect and characterize the large- and small-scale coherent structures in turbulent flow with and without RBC analogs in the absence of complex wall effects.

RESULTS AND OUTLOOK

Figure 4 shows the calibration target used to validate the optical matching between each of the three solutions and the hydrogel beads. The calibration target provides a means of confirming refractive index matching between the beads and the suspending fluid through an absence of grid distor-

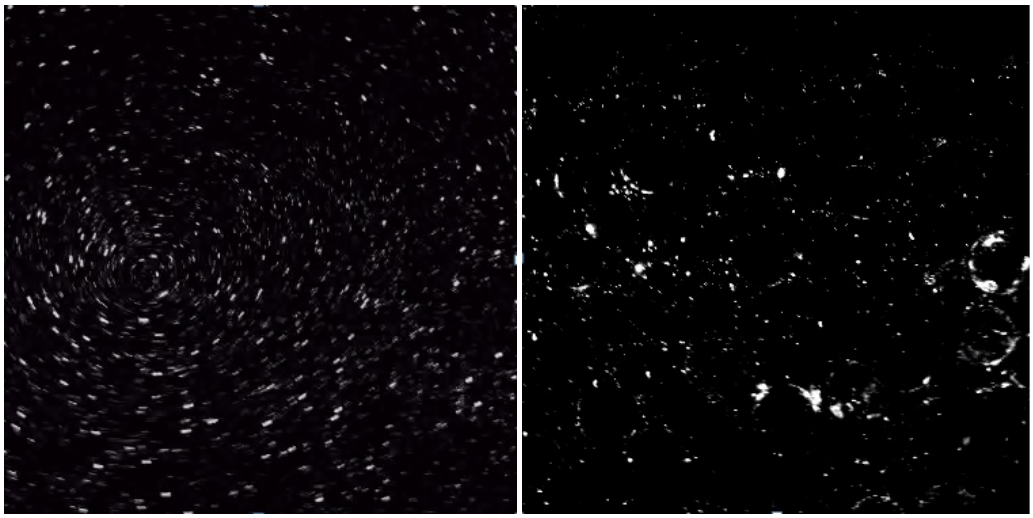

Figure 5. Raw images without (left) and with hydrogel beads (right). As shown, the addition of the beads restricts the presence of tracer particles to the empty void between the beads.

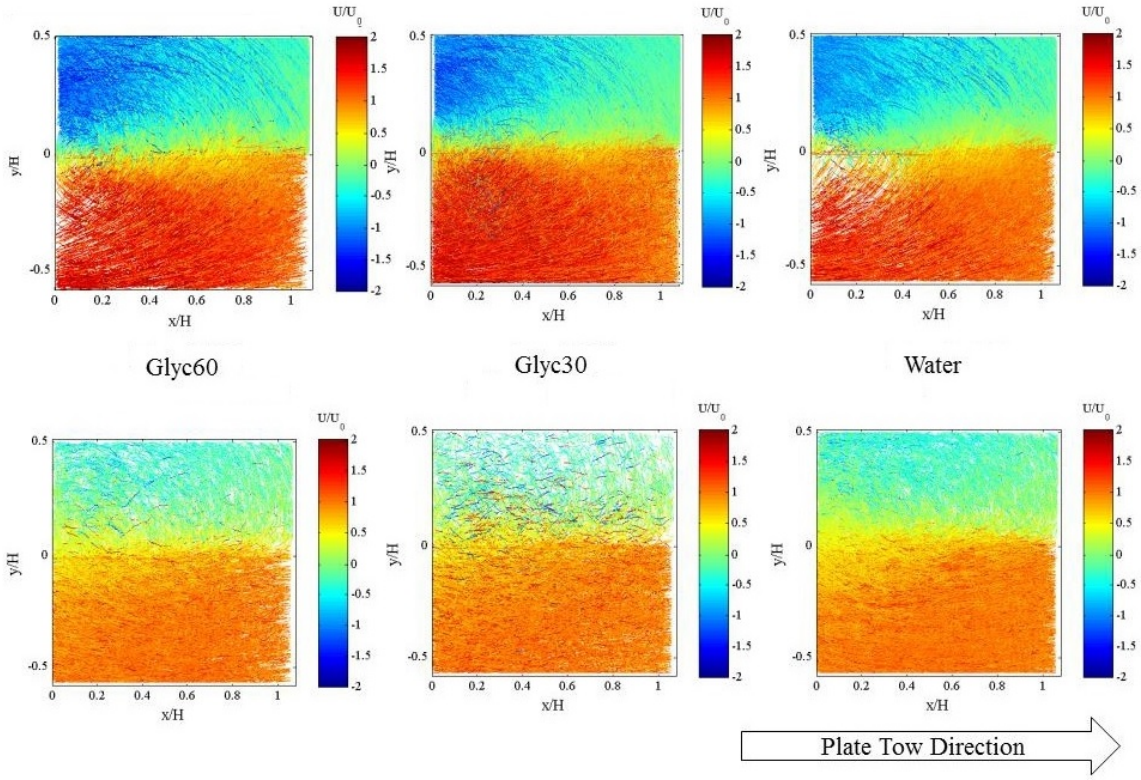

Figure 6. Lagrangian U-component velocity plots produced using data from all 20 runs for cases without beads (top) and 100 runs for cases with beads (bottom). Velocity and dimensions are normalized by the plate speed (U_0) and plate height (H), respectively. Plate tow direction is from left to right and the plate tip is at $y/H = 0$ and extends down to the x-axis.

tion. Moreover, with the glycerol solutions, optical clarity confirmed complete mixing throughout the tank. The raw images with and without beads shown in figure 5 confirms the optical quality and the ability to track seeding particles.

The Lagrangian U-component velocity plots are shown in figure 6. Although the velocity patterns are comparable in each of the three solutions, substantial differences between the velocity patterns with hydrogel beads (top row) and without (bottom row) can be observed. In the absence of the hydrogel beads, circular patterns are noticeable while these patterns become less discernible with beads. Moreover, the maximum streamwise velocity is reduced significantly in the presence of beads.

Our preliminary study confirmed adequate hydrogel optical matching and the utility of PTV application to such two-phase solutions. To build upon these results, a new

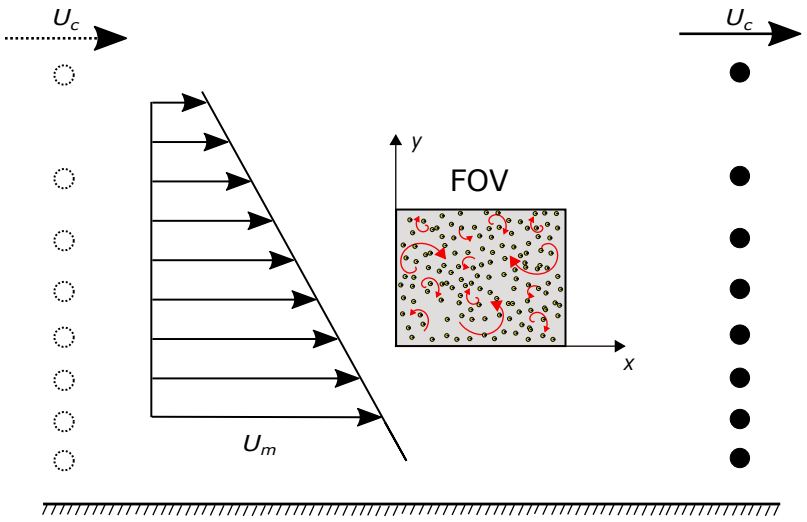

Figure 7. Side view schematic of the test section. The shear generator is passing through the field of view (FOV) with a constant velocity (U_c) and generating a uniform mean velocity gradient (dU_m/dy).

setup has been designed in order to analyze the interaction of RBC analogs with turbulent shear flow. A schematic of the shear generator passing through the field of view is shown in figure 7. A uniform mean velocity gradient can be generated at a certain distance behind the shear generator. The concept of homogeneous turbulent shear flow was first introduced by von Kármán (1937). The homogeneous single-phase turbulent shear flow has been achieved both numerically (e.g. Rogallo, 1981) and experimentally in water and wind tunnels (e.g. Rose, 1966; Tavoularis & Corrsin, 1981; Vanderwel & Tavoularis, 2011). Although this flow is theoretically simpler than traditional wall-bounded flows such as channel and boundary layer flows, it is more difficult to realize experimentally (Tavoularis & Corrsin, 1981). Nevertheless, the preliminary results with this set-up show that a uniform mean velocity gradient is attainable. The validation of the flow as well as the analysis of structures and turbulent statistics in the presence of the RBC analogs are in progress.

CONCLUSIONS

Past work has demonstrated that turbulence has significant effects on RBC hemolysis and platelet activation. On the other hand, it has been shown that particles in particle-laden flows act to either augment or attenuate turbulent kinetic energy, depending on the individual and combined properties of the particles and fluid. Hence, an important interaction between RBCs and turbulence is expected and whereupon the exploration of this interaction is the main motivation of the present research.

For this purpose, deformable hydrogel beads with a diameter of 1.0 cm were used to represent RBCs. In the preliminary experiment, hydrogel beads at a concentration of approximately 50% by volume were added to different suspending fluids. A simple shear flow was generated by towing a rectangular plate in the spanwise-wall-normal plane through quiescent fluid in a small tank. Excellent optical matching was observed between the hydrogel beads and the suspending fluids for the purpose of PTV measurements. The Lagrangian streamwise velocity plots show substantial differences between the velocity patterns with and without hydrogel beads while patterns in different solutions are comparable.

Following the preliminary experiment, a new set-up has been designed to analyze the detailed interaction of RBC analogs with turbulent shear flow. A nearly homogeneous turbulent shear flow is generated in a large-scale tank by towing a shear generator consisting of a plane parallel-rod grid of uniform rod diameter with non-uniform spacing. The turbulent statistics and turbulent coherent structures will be analyzed in the presence and absence of the RBC analogs at different shear rates. We believe that the study of such a turbulent shear flow from a structural point of view will lead to a deeper understanding of the interactions between red blood cells and turbulence.

REFERENCES

Adrian, R. J. 2007 Hairpin vortex organization in wall turbulence . *Phys. Fluids* **19** (4), 041301.

Balachandar, S. & Eaton, J. K. 2010 Turbulent dispersed multiphase flow. *Annu. Rev. Fluid Mech.* **42**, 111–133.

Bellani, G., Byron, M. L., Collignon, A. G., Meyer, C. R. & Variano, E. A. 2012 Shape effects on turbulent modulation by large nearly neutrally buoyant particles. *J. Fluid Mech.* **712**, 41–60.

Biasetti, J., Hussain, F. & Gasser, T. C. 2011 Blood flow and coherent vortices in the normal and aneurysmatic aortas: a fluid dynamical approach to intra-luminal thrombus formation. *J. R. Soc. Interface* pp. 1–13.

Bluestein, D., Gutierrez, C., Londono, M. & Schoephoerster, R. T. 1999 Vortex shedding in steady flow through a model of an arterial stenosis and its relevance to mural platelet deposition. *Ann. Biomed. Eng.* **27** (6), 763–773.

Cierpka, C., Lütke, B. & Kähler, C. J. 2013 Higher order multi-frame particle tracking velocimetry. *Exp. Fluids* **54** (5), 1–12.

Cristini, V. & Kassab, G. S. 2005 Computer modeling of red blood cell rheology in the microcirculation: a brief overview. *Ann. Biomed. Eng.* **33** (12), 1724–1727.

Fedosov, D. A., Caswell, B., Popel, A. S. & Karniadakis, G. E. 2010 Blood flow and cell-free layer in microvessels. *Microcirculation* **17** (8), 615–628.

Han, S. I., Marseille, O., Gehlen, C. & Blümich, B. 2001 Rheology of blood by nmr. *J. Magn. Reson.* **152** (1), 87–94.

Jiménez, J. 2013 Near-wall turbulence. *Phys. Fluids* **25** (10), 101302.

Kármán, T. von 1937 The fundamentals of the statistical theory of turbulence. *J . Aero. Sci.* **4**, 131.

Ku, D. N. 1997 Blood flow in arteries. *Annu. Rev. Fluid Mech.* **29** (1), 399–434.

Mansour, M. H., Bressloff, N. W. & Shearman, C. P. 2010 Red blood cell migration in microvessels. *Biorheology* **47** (1), 73–93.

Owen, P. R. & Zienkiewicz, H. K. 1957 The production of uniform shear flow in a wind tunnel. *J. Fluid Mech.* **2** (06), 521–531.

Rogallo, R. S. 1981 Numerical experiments in homogeneous turbulence. *NASA Tech. Rep.* **81**, 31508.

Rose, W. G. 1966 Results of an attempt to generate a homogeneous turbulent shear flow. *J. Fluid Mech.* **25** (01), 97–120.

Secomb, Timothy W, Styp-Rekowska, Beata & Pries, Axel R 2007 Two-dimensional simulation of red blood cell deformation and lateral migration in microvessels. *Ann. Bimed. Eng.* **35** (5), 755–765.

Shadden, S. C. & Taylor, C. A. 2008 Characterization of coherent structures in the cardiovascular system. *Ann. Biomed. Eng.* **36** (7), 1152–1162.

Stein, P. D. & Sabbah, H. N. 1976 Turbulent blood flow in the ascending aorta of humans with normal and diseased aortic valves. *Circulation research* **39** (1), 58–65.

Steinman, D. A. 2012 Assumptions in modelling of large artery hemodynamics. In *Modeling of Physiological Flows*, pp. 1–18. Springer.

Tanaka, Tomohiko & Eaton, John K 2008 Classification of turbulence modification by dispersed spheres using a novel dimensionless number. *Phys. Rev. Lett.* **101** (11), 114502.

Tavoularis, S. & Corrsin, S. 1981 Experiments in nearly homogenous turbulent shear flow with a uniform mean temperature gradient. part 1. *J. Fluid Mech.* **104**, 311–347.

Vanderwel, C. & Tavoularis, S. 2011 Coherent structures in uniformly sheared turbulent flow. *J. Fluid Mech.* **689**, 434–464.

Vétel, J., Garon, A. & Pelletier, D. 2009 Lagrangian coherent structures in the human carotid artery bifurcation. *Exp. Fluids* **46** (6), 1067–1079.

Weitzman, J. S., Samuel, L. C., Craig, A. E., Zeller, R. B., Monismith, S. G. & Koseff, J. R. 2014 On the use of refractive-index-matched hydrogel for fluid velocity measurement within and around geometrically complex solid obstructions. *Exp. Fluids* **55** (1862), 1–12.

Yen, J., Chen, S., Chern, M. & Lu, P. 2014 The effect of turbulent viscous shear stress on red blood cell hemolysis. *J. Artif. Organs* **17** (2), 178–185.